Acta Cryst E CRYSTALLOGRAPHIC COMMUNICATIONS

ISSN 2056-9890

Crystal structure, Hirshfeld surface analysis and interaction energy calculation of 4-(furan-2-yl)-2-(6-methyl-2,4-dioxopyran-3-ylidene)-2,3,4,5-tetrahydro-1*H*-1,5-benzodiazepine

Mohamed El Hafi,[a] Sanae Lahmidi,[a] Lhoussaine El Ghayati,[a] Tuncer Hökelek,[b] Joel T. Mague,[c] Bushra Amer,[d]* Nada Kheira Sebbar[a,e] and El Mokhtar Essassi[e]

[a]Laboratory of Heterocyclic Organic Chemistry, Department of Chemistry, Faculty of Sciences, Mohammed V University in Rabat, BP 1014, Rabat, Morocco, [b]Department of Physics, Hacettepe University, 06800 Beytepe, Ankara, Turkey, [c]Department of Chemistry, Tulane University, New Orleans, LA 70118, USA, [d]Faculty of Medicine and Health Sciences, Sana'a University, Sana'a, Yemen, and [e]Applied Chemistry and Environment Laboratory, Applied Bioorganic Chemistry Team, Faculty of Science, Ibn Zohr University, Agadir, Morocco. *Correspondence e-mail: Bushraamer2014@gmail.com

Received 7 June 2021
Accepted 19 July 2021

Edited by M. Weil, Vienna University of Technology, Austria

Keywords: crystal structure; pyrandione; furan; tetrahydrobenzodiazepine; hydrogen bond; π-stacking.

CCDC reference: 2097593

Supporting information: this article has supporting information at journals.iucr.org/e

The title compound {systematic name: (*S*,*E*)-3-[4-(furan-2-yl)-2,3,4,5-tetrahydro-1*H*-benzo[*b*][1,4]diazepin-2-ylidene]-6-methyl-2*H*-pyran-2,4(3*H*)-dione}, $C_{19}H_{16}N_2O_4$, is constructed from a benzodiazepine ring system linked to furan and pendant dihydropyran rings, where the benzene and furan rings are oriented at a dihedral angle of 48.7 (2)°. The pyran ring is modestly non-planar [largest deviation of 0.029 (4) Å from the least-squares plane] while the tetrahydrodiazepine ring adopts a boat conformation. The rotational orientation of the pendant dihydropyran ring is partially determined by an intramolecular $N-H_{Diazp}\cdots O_{Dhydp}$ (Diazp = diazepine and Dhydp = dihydropyran) hydrogen bond. In the crystal, layers of molecules parallel to the *bc* plane are formed by $N-H_{Diazp}\cdots O_{Dhydp}$ hydrogen bonds and slipped π–π stacking interactions. The layers are connected by additional slipped π–π stacking interactions. A Hirshfeld surface analysis of the crystal structure indicates that the most important contributions for the crystal packing are from H···H (46.8%), H···O/O···H (23.5%) and H···C/C···H (15.8%) interactions, indicating that van der Waals interactions are the dominant forces in the crystal packing. Computational chemistry indicates that in the crystal the N—H···O hydrogen-bond energy is 57.5 kJ mol^{-1}.

1. Chemical context

1,5-Benzodiazepine derivatives are an important class of nitrogen-containing heterocyclic compounds because of their potent biological activities, acting as antidepressant (Sharma *et al.*, 2017), antitubercular (Singh *et al.*, 2017), antimicrobial (An *et al.*, 2016) and anticonvulsant agents (Jyoti & Mithlesh, 2013). Many synthetic methodologies have been developed to access this type of compound (Sebhaoui *et al.*, 2017; Chkirate *et al.*, 2018).

The present study continues the investigation of 1,5-benzodiazepine derivatives recently published by our team (El Ghayati *et al.*, 2019, 2021; Essaghouani *et al.*, 2016, 2017). In this context, we report herein the synthesis, the molecular and crystal structures along with the Hirshfeld surface analysis and the intermolecular interaction energies of the title compound, (I).

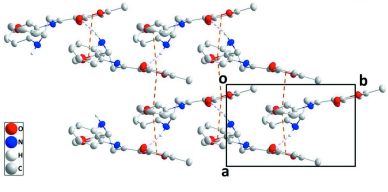

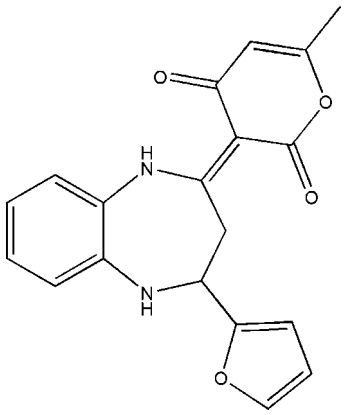

2. Structural commentary

The O1/C10–C14 pyran ring is not planar and a puckering analysis (Cremer & Pople, 1975) yielded the parameters Q = 0.082 (4) Å, θ = 114 (3)° and φ = 70 (3)°, thus indicating it adopts a slightly twisted envelope conformation with C10 at the tip of the flap. In the seven-membered ring, N1 and N2 are displaced from the C1–C6 plane by 0.159 (6) and 0.158 (6) Å, respectively, in the direction away from C8 (Fig. 1). A puckering analysis of the seven-membered ring gave the parameters $Q(2)$ = 0.915 (4) Å, $Q(3)$ = 0.187 (4) Å, $\varphi(2)$ = 38.9 (2)° and $\varphi(3)$ = 156.3 (12)° [total puckering amplitude Q = 0.933 (4) Å]. This ring adopts a boat conformation. The mean plane of the O1/C10–C14 ring is inclined to that of the C1–C6 ring by 34.8 (1)°, while the C1–C6 and O4/C16–C19 rings make a dihedral angle of 48.7 (2)°. The orientation of the O1/C10–C14 ring is partially determined by an intramolecular N1—H1···O2 hydrogen bond (Table 1, Fig. 1). All bond lengths and angles in the molecule of (I) are in the expected ranges.

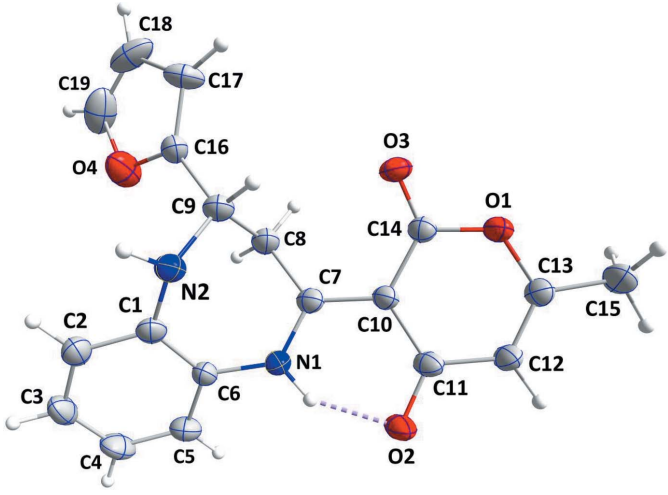

Figure 1
The molecule of (I) with the atom-numbering scheme and displacement ellipsoids drawn at the 50% probability level. The intramolecular hydrogen bond is depicted by a dashed line.

Table 1
Hydrogen-bond geometry (Å, °).

D—H···A	D—H	H···A	D···A	D—H···A
N1—H1···O2	0.91 (1)	1.72 (3)	2.538 (4)	148 (4)
N2—H2A···O3^{vi}	0.91 (1)	2.20 (2)	3.079 (4)	162 (5)

Symmetry code: (vi) $-x+1, y-\frac{1}{2}, -z+\frac{1}{2}$.

3. Supramolecular features

In the crystal, $N-H_{Diazp}\cdots O_{Dhydp}$ (Diazp = diazepine and Dhydp = dihydropyran) hydrogen bonds (Table 1) form helical chains of molecules extending along the b-axis direction. The chains are reinforced by slipped π–π stacking interactions between furan and pyran rings within the chains [centroid···centroid($-x+1, y+\frac{1}{2}, -z+\frac{1}{2}$) distance = 3.610 (2) Å, dihedral angle = 4.4 (2)°, slippage = 1.14 Å]. The chains are connected into layers parallel to the bc plane by analogous π–π stacking interactions (Fig. 2) [centroid···centroid($-x+1, y-\frac{1}{2}, -z+\frac{1}{2}$) distance = 3.610 (2) Å, dihedral angle = 4.4 (2)°, slippage = 1.38 Å]. The layers are connected by slipped π–π stacking interactions

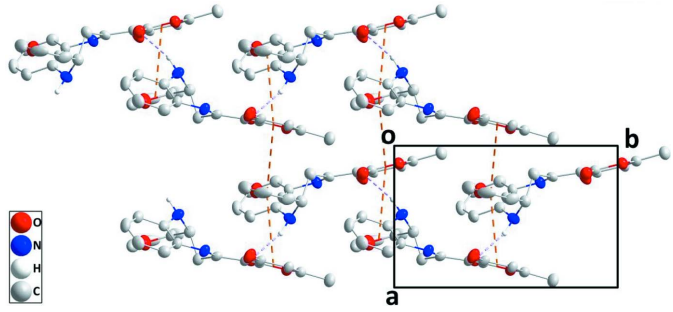

Figure 2
Portions of two chains viewed along the c axis direction with N—H···O hydrogen bonds and slipped π–π stacking interactions depicted, respectively, by violet and orange dashed lines.

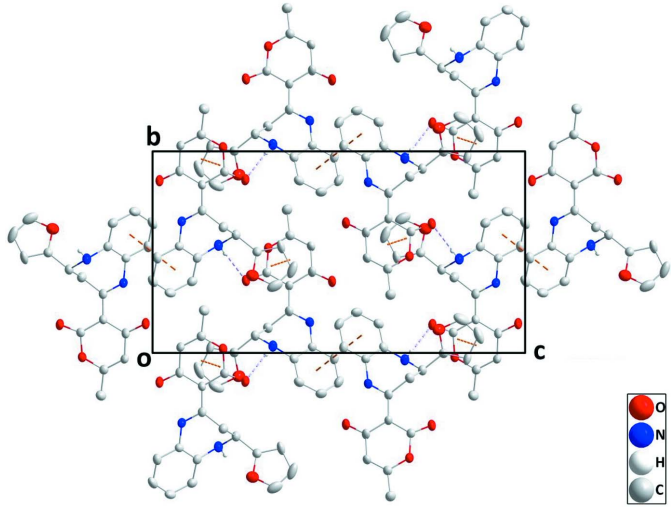

Figure 3
Packing viewed along the a-axis direction with intermolecular interactions depicted as in Fig. 2.

between inversion-related C1–C6 rings [centroid···centroid ($-x+1, -y, -z+1$) distance = 3.690 (2) Å, slippage = 1.47 Å] (Fig. 3).

4. Hirshfeld surface analysis

In order to visualize the intermolecular interactions in the crystal of (I), a Hirshfeld surface (HS) analysis (Hirshfeld, 1977) was carried out using *Crystal Explorer 17.5* (Turner *et al.*, 2017). In the HS plotted over d_{norm} (Fig. 4*a*), the white surface indicates contacts with distances equal to the sum of van der Waals radii, and the red and blue colours indicate distances shorter or longer than the van der Waals radii, respectively (Venkatesan *et al.*, 2016). The bright-red spots appearing near O3 and hydrogen atom H2*A* indicate their roles as the respective donor and/or acceptor atoms in hydrogen bonding. They also appear as blue and red regions corresponding to positive and negative potentials on the HS mapped over electrostatic potential (Spackman *et al.*, 2008; Jayatilaka *et al.*, 2005) as shown in Fig. 4*b*. The blue regions indicate the positive electrostatic potential (hydrogen-bond donors), while the red regions indicate the negative electrostatic potential (hydrogen-bond acceptors). The shape-index of the HS is a tool to visualize the π–π stacking by the presence of adjacent red and blue triangles. Fig. 4*c* clearly suggests that there are π–π interactions in (I). The overall two-dimensional fingerprint plot, Fig. 5*a*, and those delineated into H···H, H···O/O···H, H···C/C···H, C···C, H···N/N···H, C··· O/O···C and O···O contacts (McKinnon *et al.*, 2007) are illustrated in Fig. 5*b*–*h*, respectively, together with their relative contributions to the Hirshfeld surface. The most important interaction is H···H (Table 2) contributing 46.8% to the overall crystal packing, which is reflected in Fig. 5*b* as widely scattered points of high density due to the large hydrogen content of the molecule with the tip at $d_e = d_i = 1.07$ Å. The pair of scattered points of spikes in the fingerprint plot delineated into H···O/O···H contacts (23.5% contribution to the HS,Fig. 5*c*; Table 2) have the tips at $d_e + d_i = 2.09$ Å. In the absence of C—H···π interactions, the pair of characteristic wings in the fingerprint plot delineated into H···C/C···H contacts (Fig. 5*d*, 15.8%) have tips at $d_e + d_i$ = 2.95 Å. The C···C contacts (Fig. 5*e*, 7.4%) have an arrow-

Table 2
Selected interatomic distances (Å).

O2···N1	2.537 (4)	N1···N2	2.865 (4)
O3···C8	2.856 (4)	C4···C6^{iii}	3.387 (5)
O3···N2^{i}	3.079 (4)	C14···C16^{i}	3.407 (5)
O4···N2	2.955 (5)	C1···H8*A*	2.68
O2···H12^{ii}	2.74	C6···H8*A*	2.59
O2···H3^{iii}	2.62	C11···H1	2.28 (3)
O2···H1	1.72 (3)	C14···H2*A*^{i}	2.79 (4)
O3···H2*A*^{i}	2.20 (4)	C14···H8*B*	2.64
H15*C*···O3^{iv}	2.70	H2···H2*A*	2.29
O3···H2^{i}	2.68	H2···H17^{vi}	2.33
O3···H8*B*	2.23	H3···H17^{vi}	2.38
O4···H15*B*^{v}	2.70	H12···H15*A*	2.42

Symmetry codes: (i) $-x+1, y+\frac{1}{2}, -z+\frac{1}{2}$; (ii) $-x+2, -y+1, -z+1$; (iii) $-x+1, -y, -z+1$; (iv) $-x+2, y+\frac{1}{2}, -z+\frac{1}{2}$; (v) $x, y-1, z$; (vi) $-x+1, y-\frac{1}{2}, -z+\frac{1}{2}$.

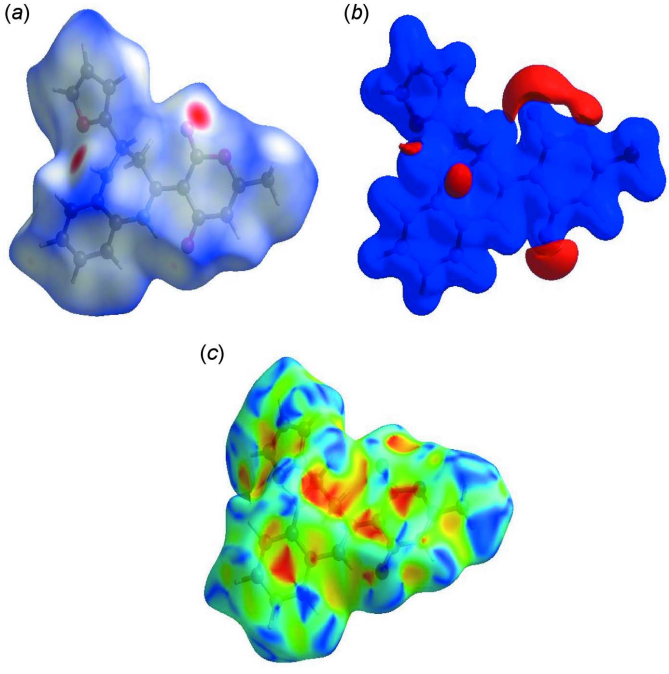

Figure 4
(*a*) View of the three-dimensional Hirshfeld surface of the title compound, plotted over d_{norm} in the range of −0.3842 to 1.4934 a.u., (*b*) view of the three-dimensional Hirshfeld surface of the title compound plotted over electrostatic potential energy in the range −0.0500 to 0.0500 a.u. using the STO-3 G basis set at the Hartree–Fock level of theory and (*c*) Hirshfeld surface of the title compound plotted over shape-index.

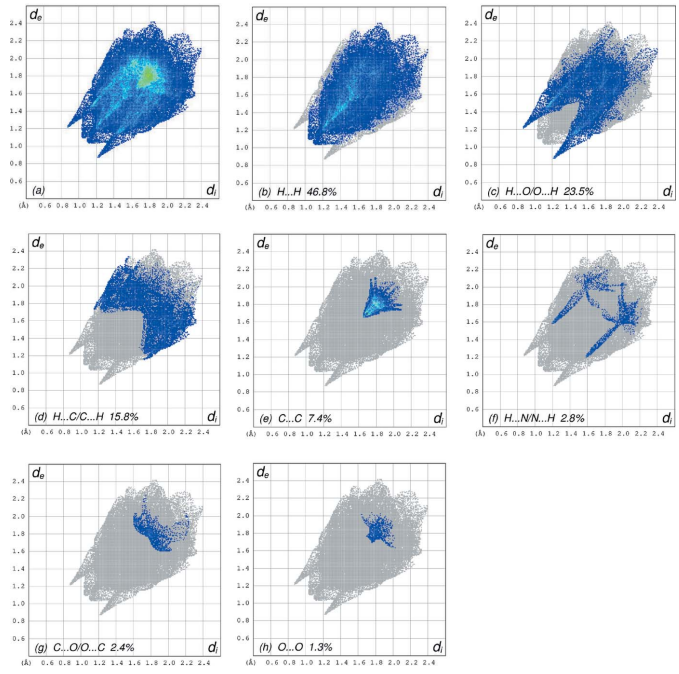

Figure 5
The full two-dimensional fingerprint plots for the title compound, showing (*a*) all interactions, and delineated into (*b*) H···H, (*c*) H···O/O···H, (*d*) H···C/C···H, (*e*) C···C, (*f*) H···N/N···H, (*g*) C···O/O···C and (*h*) O···O interactions. The d_i and d_e values are the closest internal and external distances (in Å) from given points on the Hirshfeld surface.

shaped distribution of points with its tip at $d_e = d_i = 1.65$ Å. The H···N/N···H contacts (Fig. 5*f*, 2.8%) have tips at $d_e + d_i = 2.78$ Å. Finally, the C···O/O···C (Fig. 5*g*) and O···O (Fig. 5*h*) contacts (2.4% and 1.3% contributions, respectively, to the HS) appear with tips at $d_e + d_i = 3.50$ Å and $d_e = d_i = 1.73$ Å, respectively.

The Hirshfeld surface representations with the function d_{norm} plotted onto the surface are shown for the H···H, H···O/O···H, H···C/C···H and C···C interactions in Fig. 6*a*–*d*, respectively.

The Hirshfeld surface analysis confirms the importance of H-atom contacts in establishing the packing. The large number of H···H, H···O/O···H, and H···C/C···H interactions suggest that van der Waals interactions play the major role in the crystal packing (Hathwar *et al.*, 2015).

5. Interaction energy calculations

The intermolecular interaction energies were calculated using the CE–B3LYP/6–31G(d,p) energy model available in *Crystal Explorer 17.5* (Turner *et al.*, 2017), where a cluster of molecules is generated by applying crystallographic symmetry operations with respect to a selected central molecule within the default radius of 3.8 Å (Turner *et al.*, 2014). The total intermolecular energy (E_{tot}) is the sum of electrostatic (E_{ele}), polarization (E_{pol}), dispersion (E_{dis}) and exchange-repulsion (E_{rep}) energies (Turner *et al.*, 2015) with scale factors of 1.057, 0.740, 0.871 and 0.618, respectively (Mackenzie *et al.*, 2017). The hydrogen bonding interaction energy for the N2—H2*A*···O3 hydrogen bond was calculated (in kJ mol^{-1}) as −32.6 (E_{ele}), −7.4 (E_{pol}), −60.8 (E_{dis}), 57.3 (E_{rep}) and −57.5 (E_{tot}).

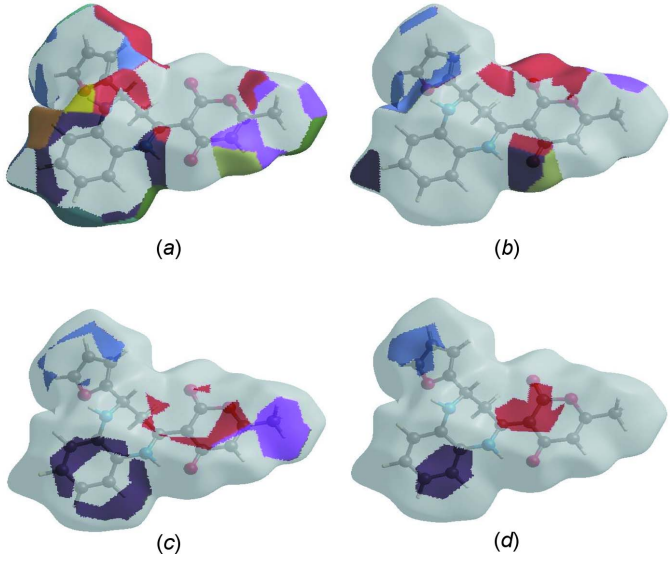

Figure 6
The Hirshfeld surface representations with the function d_{norm} plotted onto the surface for (*a*) H···H, (*b*) H···O/O···H, (*c*) H···C/C···H and (*d*) C···C interactions.

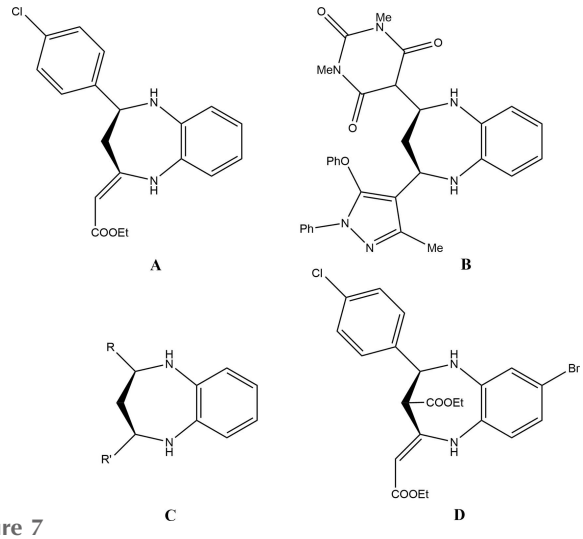

Figure 7
Diagrams of compounds structurally related to (I).

6. Database survey

A search of the Cambridge Structural Database (CSD, updated 29 May 2021; Groom *et al.*, 2016) for 2,3,4,5-tetrahydro-1*H*benzo[*b*][1,4] diazepines substituted at the 2- and 4-positions gave a substantial number of hits with seven deemed closely similar to the title molecule (Fig. 7). These are: **A** (Lal *et al.*, 2013), **B** (Siddiqui & Siddiqui, 2020), **C** with R = 4-ClC$_6$H$_4$, thiophene, 3,4-(MeO)C$_6$H$_3$ and R' = 6- methyl-2*H*-pyran-2,4-(3*H*)-dione as well as R = 6-methyl-2*H*- pyran-2,4-(3*H*)-dione and R' = 3-BrC$_6$H$_4$ (Faidallah *et al.*, 2015) and **D** (Wu & Wang, 2020) (Fig. 7). All have the tetrahydrodiazepine ring adopting a boat conformation with puckering amplitudes in the range 0.702 (2) Å (for **A**) to 0.957 (2) Å (for **C**, R = thiophene). The dihedral angles between the mean planes of the benzo rings and those of the ring-containing substituents on the seven-membered ring vary considerably, likely due to packing considerations as the steric bulk of these groups differ markedly.

7. Synthesis and crystallization

To a suspension of 3-[1-(2-aminophenylimino)ethyl]-4-hydroxy-6-methylpyran-2-one (4 mmol) in ethanol (40 ml) were added 1.5 equivalents of furan-2-carboxaldehyde and four drops of trifluoroacetic acid (TFA). The mixture was refluxed for 3 h. Cooling to room temperature induced the precipitation of a yellow solid, which was filtered off, and then washed with 20 ml of cold ethanol. Crystals suitable for X-ray analysis were obtained by recrystallization of the bulk from ethanol solution to afford colourless crystals (yield: 75%).

8. Refinement

Crystal, data collection and refinement details are presented in Table 3. Inspection of the data with *CELL_NOW* (Sheldrick, 2009) revealed that the crystal under investigation was twinned by a 180° rotation about the *a** axis with a subse-

quently refined 78:22 ratio of the two twin components. The full two-component reflection file (HKLF-5 format) was used for the final refinement. Hydrogen atoms attached to carbon were included as riding contributions in idealized positions (C—H = 0.95–0.99 Å) with U_{iso}(H) = 1.2–1.5U_{eq}(C). Those attached to nitrogen were restrained to a target bond length of 0.91 Å using the DFIX instruction in *SHELXL*. The displacement ellipsoids of the O1/C10–C14 ring suggest a possible slight disorder in this group, but it does not appear large enough to model with alternate locations of the atoms.

Acknowledgements

Authors' contributions are as follows. Conceptualization,MEH, SL, LEG and NKS; methodology, BA and MEH; investigation, MEH,JTM and TH; writing (original draft), JTM, TH and NKS; writing (review and editing of the manuscript), MEH, SL and LEG; visualization, NKS and EME; resources, EME and MEH; supervision, BA and NKS.

Funding information

JTM thanks Tulane University for support of the Tulane Crystallography Laboratory. TH is grateful to Hacettepe University Scientific Research Project Unit (grant No. 013 D04 602 004).

Table 3
Experimental details.

Crystal data	
Chemical formula	$C_{19}H_{16}N_2O_4$
M_r	336.34
Crystal system, space group	Monoclinic, $P2_1/c$
Temperature (K)	150
a, b, c (Å)	7.0111 (8), 11.0123 (13), 20.493 (2)
β (°)	96.202 (5)
V (Å^3)	1573.0 (3)
Z	4
Radiation type	Mo $K\alpha$
μ (mm^{-1})	0.10
Crystal size (mm)	0.34 × 0.22 × 0.11
Data collection	
Diffractometer	Bruker D8 QUEST PHOTON 3 diffractometer
Absorption correction	Multi-scan (*TWINABS*; Sheldrick, 2009)
T_{min}, T_{max}	0.97, 0.99
No. of measured, independent and observed [$I > 2\sigma(I)$] reflections	5201, 5201, 4007
R_{int}	0.081
(sin $\theta/\lambda)_{max}$ (Å^{-1})	0.672
Refinement	
$R[F^2 > 2\sigma(F^2)]$, $wR(F^2)$, S	0.079, 0.214, 1.14
No. of reflections	5201
No. of parameters	236
No. of restraints	2
H-atom treatment	H atoms treated by a mixture of independent and constrained refinement
$\Delta\rho_{max}$, $\Delta\rho_{min}$ (e Å^{-3})	0.54, −0.30

Computer programs: *APEX3* and *SAINT* (Bruker, 2020), *SHELXT* (Sheldrick, 2015*a*), *SHELXL2018/1* (Sheldrick, 2015*b*), *DIAMOND* (Brandenburg & Putz, 2012) and *publCIF* (Westrip, 2010).

References

An, Y. S., Hao, Z. F., Zhang, X. J. & Wang, L. Z. (2016). *Chem. Biol. Drug Des.* **88**, 110–121.
Brandenburg, K. & Putz, H. (2012). *DIAMOND*, Crystal Impact GbR, Bonn, Germany.
Bruker (2020). *APEX3* and *SAINT*. Madison, WI. Bruker AXS Inc., Madison, Wisconsin, USA.
Chkirate, K., Sebbar, N. K., Karrouchi, K. & Essassi, E. M. (2018). *J. Mar. Chim. Heterocycl*, **17**, 1–27.
Cremer, D. & Pople, J. A. (1975). *J. Am. Chem. Soc.* **97**, 1354–1358.
El Ghayati, L., Ramli, Y., Hökelek, T., Labd Taha, M., Mague, J. T. & Essassi, E. M. (2019). *Acta Cryst.* E**75**, 94–98.
El Ghayati, L., Sert, Y., Sebbar, N. K., Ramli, Y., Ahabchane, N. H., Talbaoui, A., Mague, J. T., El Ibrahimi, B., Taha, M. L., Essassi, E. M., Al–Zaqri, N. & Alsalme, A. (2021). *J. Heterocycl. Chem.* **58**, 270–289.
Essaghouani, A., Boulhaoua, M., El Hafi, M., Benchidmi, M., Essassi, E. M. & Mague, J. T. (2017). *IUCrData*, **2**, x170120.
Essaghouani, A., Elmsellem, H., Boulhaoua, M., Ellouz, M., El Hafi, M., Sebbar, N. K., Essassi, E. M., Bouabdellaoui, M., Aouniti, A. & Hammouti, B. (2016). *Pharma Chemica*, **8**, 347–355.
Faidallah, H. M., Taib, L. A., Albeladi, S. N. A., Rahman, M. E. U., Al-Zahrani, F. A., Arshad, M. N. & Asiri, A. M. (2015). *J. Chem. Res.* **39**, 502–508.
Groom, C. R., Bruno, I. J., Lightfoot, M. P. & Ward, S. C. (2016). *Acta Cryst.* B**72**, 171–179.
Hathwar, V. R., Sist, M., Jørgensen, M. R. V., Mamakhel, A. H., Wang, X., Hoffmann, C. M., Sugimoto, K., Overgaard, J. & Iversen, B. B. (2015). *IUCrJ*, **2**, 563–574.
Hirshfeld, H. L. (1977). *Theor. Chim. Acta*, **44**, 129–138.
Jayatilaka, D., Grimwood, D. J., Lee, A., Lemay, A., Russel, A. J., Taylor, C., Wolff, S. K., Cassam-Chenai, P. & Whitton, A. (2005). *TONTO*. Available at: http://dylan-jayatilaka.net/tonto
Jyoti, Y. & Mithlesh, P. D. (2013). *Pharm. Sin.* **4**, 81–90.
Lal, M., Basha, R. S., Sarkar, S. & Khan, A. T. (2013). *Tetrahedron Lett.* **54**, 4264–4272.
Mackenzie, C. F., Spackman, P. R., Jayatilaka, D. & Spackman, M. A. (2017). *IUCrJ*, **4**, 575–587.
McKinnon, J. J., Jayatilaka, D. & Spackman, M. A. (2007). *Chem. Commun.* pp. 3814–3816.
Sebhaoui, J., El Bakri, Y., Essassi, E. M. & Mague, J. T. (2017). *IUCrData*, **2**, x171057.
Sharma, R., Tilak, A., Thakur, R. N., Gangwar, S. S. & Sutar, R. C. (2017). *World J. Pharm. Res.* **6**, 925–931.
Sheldrick, G. M. (2009). *TWINABS* and *CELL_NOW*. University of Göttingen, Göttingen, Germany.
Sheldrick, G. M. (2015*a*). *Acta Cryst.* A**71**, 3–8.
Sheldrick, G. M. (2015*b*). *Acta Cryst.* C**71**, 3–8.
Siddiqui, S. & Siddiqui, Z. N. (2020). *Nanoscale Advance* **2**, 4639–4651.
Singh, G., Nayak, S. K. & Monga, V. (2017). *Indian J. Heterocycl. Chem.* **27**, 143–149.
Spackman, M. A., McKinnon, J. J. & Jayatilaka, D. (2008). *CrystEngComm*, **10**, 377–388.
Turner, M. J., Grabowsky, S., Jayatilaka, D. & Spackman, M. A. (2014). *J. Phys. Chem. Lett.* **5**, 4249–4255.
Turner, M. J., McKinnon, J. J., Wolff, S. K., Grimwood, D. J., Spackman, P. R., Jayatilaka, D. & Spackman, M. A. (2017). *CrystalExplorer17*. The University of Western Australia.
Turner, M. J., Thomas, S. P., Shi, M. W., Jayatilaka, D. & Spackman, M. A. (2015). *Chem. Commun.* **51**, 3735–3738.
Venkatesan, P., Thamotharan, S., Ilangovan, A., Liang, H. & Sundius, T. (2016). *Spectrochim. Acta Part A*, **153**, 625–636.
Westrip, S. P. (2010). *J. Appl. Cryst.* **43**, 920–925.
Wu, H. T. & Wang, L. Z. (2020). *New J. Chem.* **44**, 10428–10440.

supporting information

Acta Cryst. (2021). E**77**, 834-838 [https://doi.org/10.1107/S2056989021007441]

Crystal structure, Hirshfeld surface analysis and interaction energy calculation of 4-(furan-2-yl)-2-(6-methyl-2,4-dioxopyran-3-ylidene)-2,3,4,5-tetrahydro-1*H*-1,5-benzodiazepine

Mohamed El Hafi, Sanae Lahmidi, Lhoussaine El Ghayati, Tuncer Hökelek, Joel T. Mague, Bushra Amer, Nada Kheira Sebbar and El Mokhtar Essassi

Computing details

Data collection: *APEX3* (Bruker, 2020); cell refinement: *SAINT* (Bruker, 2020); data reduction: *SAINT* (Bruker, 2020); program(s) used to solve structure: *SHELXT* (Sheldrick, 2015*a*); program(s) used to refine structure: *SHELXL2018/1* (Sheldrick, 2015*b*); molecular graphics: *DIAMOND* (Brandenburg & Putz, 2012); software used to prepare material for publication: *publCIF* (Westrip, 2010).

(*S*,*E*)-3-[4-(Furan-2-yl)-2,3,4,5-tetrahydro-1*H*-benzo[*b*][1,4]diazepin-2-ylidene]-6-methyl-2*H*-pyran-2,4(3*H*)-dione

Crystal data

$C_{19}H_{16}N_2O_4$
M_r = 336.34
Monoclinic, $P2_1/c$
a = 7.0111 (8) Å
b = 11.0123 (13) Å
c = 20.493 (2) Å
β = 96.202 (5)°
V = 1573.0 (3) Å^3
Z = 4
$F(000)$ = 704
D_x = 1.420 Mg m^{-3}
Mo $K\alpha$ radiation, λ = 0.71073 Å
Cell parameters from 9980 reflections
θ = 2.7–28.4°
μ = 0.10 mm^{-1}
T = 150 K
Block, colourless
0.34 × 0.22 × 0.11 mm

Data collection

Bruker D8 QUEST PHOTON 3 diffractometer
Radiation source: fine-focus sealed tube
Graphite monochromator
Detector resolution: 7.3910 pixels mm^{-1}
φ and ω scans
Absorption correction: multi-scan (*TWINABS*; Sheldrick, 2009)
T_{min} = 0.97, T_{max} = 0.99
5201 measured reflections
5201 independent reflections
4007 reflections with $I > 2\sigma(I)$
R_{int} = 0.081
θ_{max} = 28.5°, θ_{min} = 2.7°
h = −9→9
k = 0→14
l = 0→27

Refinement

Refinement on F^2
Least-squares matrix: full
$R[F^2 > 2\sigma(F^2)]$ = 0.079
$wR(F^2)$ = 0.214
S = 1.14
5201 reflections
236 parameters
2 restraints

Primary atom site location: dual
Secondary atom site location: difference Fourier map
Hydrogen site location: mixed
H atoms treated by a mixture of independent and constrained refinement

$w = 1/[\sigma^2(F_o^2) + (0.0648P)^2 + 2.9838P]$ where $P = (F_o^2 + 2F_c^2)/3$
$(\Delta/\sigma)_{max} < 0.001$
$\Delta\rho_{max} = 0.54$ e Å^{-3}
$\Delta\rho_{min} = -0.30$ e Å^{-3}

Special details

Experimental. The diffraction data were obtained from 9 sets of frames, each of width 0.5° in ω or φ, collected with scan parameters determined by the "strategy" routine in *APEX3*. The scan time was 20 sec/frame. Analysis of 2110 reflections having I/σ(I) > 15 and chosen from the full data set with *CELL_NOW* (Sheldrick, 2008) showed the crystal to belong to the monoclinic system and to be twinned by a 180° rotation about the *a* axis. The raw data were processed using the multi-component version of *SAINT* under control of the two-component orientation file generated by *CELL_NOW*.

Geometry. All esds (except the esd in the dihedral angle between two l.s. planes) are estimated using the full covariance matrix. The cell esds are taken into account individually in the estimation of esds in distances, angles and torsion angles; correlations between esds in cell parameters are only used when they are defined by crystal symmetry. An approximate (isotropic) treatment of cell esds is used for estimating esds involving l.s. planes.

Refinement. Refinement of F^2 against ALL reflections. The weighted R-factor wR and goodness of fit S are based on F^2, conventional R-factors R are based on F, with F set to zero for negative F^2. The threshold expression of $F^2 > 2$sigma(F^2) is used only for calculating R-factors(gt) etc. and is not relevant to the choice of reflections for refinement. R-factors based on F^2 are statistically about twice as large as those based on F, and R- factors based on ALL data will be even larger. H-atoms attached to carbon were placed in calculated positions (C—H = 0.95 - 0.99 Å) and were included as riding contributions with isotropic displacement parameters 1.2 - 1.5 times those of the attached atoms. Those attached to nitrogen were placed in locations derived from a difference map and refined with a DFIX 0.91 0.01 instruction. Refined as a 2-component twin.

Fractional atomic coordinates and isotropic or equivalent isotropic displacement parameters (Å^2)

	x	*y*	*z*	U_{iso}*/U_{eq}
O1	0.8749 (4)	0.5209 (2)	0.31078 (12)	0.0307 (6)
O2	0.7779 (4)	0.3547 (3)	0.48140 (13)	0.0386 (7)
O3	0.8042 (4)	0.3592 (3)	0.25076 (12)	0.0348 (7)
O4	0.6845 (5)	−0.1158 (3)	0.23160 (17)	0.0516 (9)
N1	0.7413 (5)	0.1528 (3)	0.42168 (15)	0.0309 (7)
H1	0.750 (7)	0.206 (3)	0.4557 (16)	0.052 (14)*
N2	0.4861 (5)	0.0341 (3)	0.32311 (16)	0.0325 (8)
H2A	0.381 (5)	−0.006 (4)	0.305 (2)	0.066 (17)*
C1	0.5648 (5)	−0.0283 (3)	0.37991 (18)	0.0293 (8)
C2	0.5022 (6)	−0.1448 (4)	0.3935 (2)	0.0346 (9)
H2	0.417357	−0.185984	0.361639	0.042*
C3	0.5608 (7)	−0.2015 (4)	0.4524 (2)	0.0410 (11)
H3	0.515597	−0.280802	0.460548	0.049*
C4	0.6847 (7)	−0.1440 (4)	0.4995 (2)	0.0422 (11)
H4	0.726016	−0.183596	0.539729	0.051*
C5	0.7479 (6)	−0.0280 (4)	0.48747 (19)	0.0350 (9)
H5	0.831745	0.012667	0.519869	0.042*
C6	0.6895 (6)	0.0296 (3)	0.42827 (18)	0.0278 (8)
C7	0.7802 (5)	0.2070 (3)	0.36688 (18)	0.0270 (8)
C8	0.8001 (6)	0.1246 (4)	0.30983 (19)	0.0342 (9)
H8A	0.873700	0.051597	0.325464	0.041*

H8B	0.873351	0.167001	0.277963	0.041*
C9	0.6076 (6)	0.0860 (4)	0.27573 (19)	0.0322 (9)
H9	0.541795	0.160745	0.256997	0.039*
C10	0.8108 (5)	0.3343 (3)	0.36710 (17)	0.0261 (8)
C11	0.8122 (5)	0.4025 (3)	0.42765 (18)	0.0288 (8)
C12	0.8580 (5)	0.5294 (3)	0.42500 (18)	0.0292 (8)
H12	0.864632	0.576254	0.464103	0.035*
C13	0.8913 (6)	0.5830 (3)	0.36913 (19)	0.0290 (8)
C14	0.8277 (5)	0.3984 (3)	0.30673 (18)	0.0264 (8)
C15	0.9490 (7)	0.7108 (4)	0.3614 (2)	0.0390 (10)
H15A	0.967050	0.750057	0.404507	0.058*
H15B	0.848667	0.753521	0.333246	0.058*
H15C	1.069420	0.713570	0.341196	0.058*
C16	0.6325 (6)	0.0022 (3)	0.21928 (19)	0.0305 (8)
C17	0.6236 (6)	0.0268 (4)	0.15511 (18)	0.0382 (10)
H17	0.594168	0.102485	0.134101	0.046*
C18	0.6687 (7)	−0.0869 (5)	0.1245 (2)	0.0530 (14)
H18	0.671856	−0.100553	0.078868	0.064*
C19	0.7044 (7)	−0.1673 (5)	0.1713 (3)	0.0563 (14)
H19	0.739039	−0.249397	0.164714	0.068*

Atomic displacement parameters (Å²)

	U^{11}	U^{22}	U^{33}	U^{12}	U^{13}	U^{23}
O1	0.0372 (16)	0.0320 (14)	0.0233 (13)	−0.0023 (12)	0.0052 (11)	0.0010 (11)
O2	0.0556 (18)	0.0400 (16)	0.0201 (13)	−0.0164 (14)	0.0036 (12)	−0.0005 (12)
O3	0.0434 (17)	0.0393 (16)	0.0213 (13)	0.0028 (13)	0.0017 (12)	−0.0026 (11)
O4	0.063 (2)	0.0425 (18)	0.052 (2)	0.0052 (16)	0.0182 (17)	0.0024 (16)
N1	0.0393 (19)	0.0303 (17)	0.0230 (16)	−0.0078 (15)	0.0023 (14)	−0.0018 (13)
N2	0.0335 (19)	0.0390 (19)	0.0253 (16)	−0.0079 (15)	0.0038 (14)	0.0006 (14)
C1	0.032 (2)	0.032 (2)	0.0263 (19)	−0.0001 (17)	0.0106 (16)	−0.0033 (16)
C2	0.040 (2)	0.031 (2)	0.034 (2)	−0.0042 (18)	0.0112 (18)	−0.0050 (17)
C3	0.057 (3)	0.028 (2)	0.042 (2)	−0.005 (2)	0.022 (2)	0.0029 (18)
C4	0.055 (3)	0.043 (2)	0.031 (2)	0.007 (2)	0.013 (2)	0.0119 (19)
C5	0.039 (2)	0.042 (2)	0.0250 (19)	0.0008 (19)	0.0062 (17)	0.0020 (17)
C6	0.034 (2)	0.0257 (18)	0.0252 (18)	−0.0027 (16)	0.0093 (15)	−0.0001 (15)
C7	0.0247 (19)	0.0323 (19)	0.0238 (18)	−0.0049 (16)	0.0020 (15)	−0.0009 (15)
C8	0.041 (2)	0.034 (2)	0.030 (2)	−0.0044 (18)	0.0093 (17)	−0.0025 (17)
C9	0.038 (2)	0.034 (2)	0.0251 (19)	−0.0018 (18)	0.0073 (16)	−0.0003 (16)
C10	0.029 (2)	0.0281 (18)	0.0213 (17)	−0.0044 (15)	0.0037 (15)	0.0008 (14)
C11	0.030 (2)	0.034 (2)	0.0218 (18)	−0.0079 (16)	0.0009 (15)	−0.0001 (15)
C12	0.036 (2)	0.0288 (19)	0.0227 (18)	−0.0055 (16)	0.0021 (15)	−0.0031 (15)
C13	0.030 (2)	0.0299 (19)	0.0277 (19)	−0.0011 (16)	0.0040 (16)	−0.0011 (15)
C14	0.0254 (19)	0.0285 (19)	0.0253 (18)	−0.0006 (15)	0.0027 (15)	0.0005 (15)
C15	0.049 (3)	0.034 (2)	0.035 (2)	−0.004 (2)	0.014 (2)	0.0023 (18)
C16	0.034 (2)	0.0289 (19)	0.0282 (19)	−0.0054 (17)	0.0044 (16)	−0.0004 (16)
C17	0.036 (2)	0.056 (3)	0.0219 (19)	0.008 (2)	0.0042 (17)	0.0102 (18)
C18	0.033 (3)	0.090 (4)	0.035 (2)	−0.003 (3)	0.003 (2)	−0.026 (3)

C19	0.048 (3)	0.047 (3)	0.078 (4)	−0.003 (2)	0.025 (3)	−0.023 (3)

Geometric parameters (Å, º)

O1—C13	1.372 (4)	C7—C10	1.419 (5)
O1—C14	1.389 (4)	C7—C8	1.498 (5)
O2—C11	1.267 (4)	C8—C9	1.513 (6)
O3—C14	1.220 (4)	C8—H8A	0.9900
O4—C16	1.366 (5)	C8—H8B	0.9900
O4—C19	1.380 (6)	C9—C16	1.504 (5)
N1—C7	1.326 (5)	C9—H9	1.0000
N1—C6	1.415 (5)	C10—C14	1.440 (5)
N1—H1	0.912 (12)	C10—C11	1.449 (5)
N2—C1	1.412 (5)	C11—C12	1.436 (5)
N2—C9	1.474 (5)	C12—C13	1.331 (5)
N2—H2A	0.906 (12)	C12—H12	0.9500
C1—C2	1.393 (5)	C13—C15	1.477 (5)
C1—C6	1.402 (5)	C15—H15A	0.9800
C2—C3	1.382 (6)	C15—H15B	0.9800
C2—H2	0.9500	C15—H15C	0.9800
C3—C4	1.381 (6)	C16—C17	1.338 (5)
C3—H3	0.9500	C17—C18	1.451 (7)
C4—C5	1.383 (6)	C17—H17	0.9500
C4—H4	0.9500	C18—C19	1.309 (7)
C5—C6	1.391 (5)	C18—H18	0.9500
C5—H5	0.9500	C19—H19	0.9500
O2···C3^{i}	3.322 (5)	C3···C15^{v}	3.591 (6)
O2···N1	2.537 (4)	C4···C6^{i}	3.387 (5)
O2···C12^{ii}	3.282 (4)	C10···C18^{iii}	3.497 (6)
O3···C9	3.372 (4)	C11···C17^{iii}	3.600 (5)
O3···C8	2.856 (4)	C11···C18^{iii}	3.428 (5)
O3···N2^{iii}	3.079 (4)	C12···C12^{ii}	3.541 (5)
O4···N2	2.955 (5)	C12···C17^{iii}	3.589 (5)
O4···C1	3.376 (5)	C14···C16^{iii}	3.407 (5)
O1···H2A^{iii}	2.84 (4)	C1···H8A	2.68
O2···H12^{ii}	2.74	C2···H17^{vi}	2.91
O2···H3^{i}	2.62	C3···H17^{vi}	2.93
O2···H1	1.72 (3)	C6···H8A	2.59
O3···H9	2.87	C11···H1	2.28 (3)
O3···H2A^{iii}	2.20 (4)	C14···H2A^{iii}	2.79 (4)
H15C···O3^{iv}	2.70	C14···H8B	2.64
O3···H2^{iii}	2.68	H2···H2A	2.29
O3···H8B	2.23	H2···H17^{vi}	2.33
O4···H8A	2.88	H3···H17^{vi}	2.38
O4···H15B^{v}	2.70	H5···H1	2.55
N1···N2	2.865 (4)	H12···H15A	2.42
N2···H19^{iii}	2.89		

C13—O1—C14	122.3 (3)	C16—C9—C8	110.8 (3)
C16—O4—C19	106.0 (4)	N2—C9—H9	107.3
C7—N1—C6	126.2 (3)	C16—C9—H9	107.3
C7—N1—H1	111 (3)	C8—C9—H9	107.3
C6—N1—H1	123 (3)	C7—C10—C14	120.5 (3)
C1—N2—C9	122.0 (3)	C7—C10—C11	120.1 (3)
C1—N2—H2A	109 (3)	C14—C10—C11	119.2 (3)
C9—N2—H2A	115 (3)	O2—C11—C12	120.1 (3)
C2—C1—C6	117.6 (4)	O2—C11—C10	123.0 (3)
C2—C1—N2	120.6 (4)	C12—C11—C10	116.9 (3)
C6—C1—N2	121.3 (3)	C13—C12—C11	121.7 (3)
C3—C2—C1	121.4 (4)	C13—C12—H12	119.2
C3—C2—H2	119.3	C11—C12—H12	119.2
C1—C2—H2	119.3	C12—C13—O1	121.5 (3)
C4—C3—C2	120.6 (4)	C12—C13—C15	126.2 (4)
C4—C3—H3	119.7	O1—C13—C15	112.3 (3)
C2—C3—H3	119.7	O3—C14—O1	114.0 (3)
C3—C4—C5	119.3 (4)	O3—C14—C10	128.3 (3)
C3—C4—H4	120.4	O1—C14—C10	117.7 (3)
C5—C4—H4	120.4	C13—C15—H15A	109.5
C4—C5—C6	120.5 (4)	C13—C15—H15B	109.5
C4—C5—H5	119.8	H15A—C15—H15B	109.5
C6—C5—H5	119.8	C13—C15—H15C	109.5
C5—C6—C1	120.8 (4)	H15A—C15—H15C	109.5
C5—C6—N1	117.8 (3)	H15B—C15—H15C	109.5
C1—C6—N1	121.1 (3)	C17—C16—O4	111.0 (4)
N1—C7—C10	119.1 (3)	C17—C16—C9	129.4 (4)
N1—C7—C8	115.7 (3)	O4—C16—C9	119.5 (3)
C10—C7—C8	125.0 (3)	C16—C17—C18	105.1 (4)
C7—C8—C9	112.2 (3)	C16—C17—H17	127.4
C7—C8—H8A	109.2	C18—C17—H17	127.4
C9—C8—H8A	109.2	C19—C18—C17	107.5 (4)
C7—C8—H8B	109.2	C19—C18—H18	126.3
C9—C8—H8B	109.2	C17—C18—H18	126.3
H8A—C8—H8B	107.9	C18—C19—O4	110.4 (4)
N2—C9—C16	113.1 (3)	C18—C19—H19	124.8
N2—C9—C8	110.8 (3)	O4—C19—H19	124.8

C9—N2—C1—C2	−126.6 (4)	C7—C10—C11—O2	−3.5 (6)
C9—N2—C1—C6	61.5 (5)	C14—C10—C11—O2	172.3 (4)
C6—C1—C2—C3	−0.2 (6)	C7—C10—C11—C12	175.6 (3)
N2—C1—C2—C3	−172.4 (4)	C14—C10—C11—C12	−8.6 (5)
C1—C2—C3—C4	−0.3 (6)	O2—C11—C12—C13	−178.7 (4)
C2—C3—C4—C5	0.8 (7)	C10—C11—C12—C13	2.2 (6)
C3—C4—C5—C6	−0.8 (6)	C11—C12—C13—O1	3.1 (6)
C4—C5—C6—C1	0.4 (6)	C11—C12—C13—C15	−176.7 (4)
C4—C5—C6—N1	173.1 (4)	C14—O1—C13—C12	−1.7 (6)

C2—C1—C6—C5	0.1 (5)	C14—O1—C13—C15	178.1 (3)
N2—C1—C6—C5	172.2 (4)	C13—O1—C14—O3	174.5 (3)
C2—C1—C6—N1	−172.3 (3)	C13—O1—C14—C10	−4.9 (5)
N2—C1—C6—N1	−0.2 (5)	C7—C10—C14—O3	6.4 (6)
C7—N1—C6—C5	147.3 (4)	C11—C10—C14—O3	−169.4 (4)
C7—N1—C6—C1	−40.0 (6)	C7—C10—C14—O1	−174.3 (3)
C6—N1—C7—C10	173.6 (4)	C11—C10—C14—O1	9.9 (5)
C6—N1—C7—C8	−10.1 (6)	C19—O4—C16—C17	−1.4 (5)
N1—C7—C8—C9	79.4 (4)	C19—O4—C16—C9	−177.3 (4)
C10—C7—C8—C9	−104.5 (4)	N2—C9—C16—C17	135.7 (4)
C1—N2—C9—C16	94.4 (4)	C8—C9—C16—C17	−99.2 (5)
C1—N2—C9—C8	−30.7 (5)	N2—C9—C16—O4	−49.3 (5)
C7—C8—C9—N2	−52.9 (4)	C8—C9—C16—O4	75.8 (5)
C7—C8—C9—C16	−179.3 (3)	O4—C16—C17—C18	1.8 (5)
N1—C7—C10—C14	−171.6 (4)	C9—C16—C17—C18	177.1 (4)
C8—C7—C10—C14	12.4 (6)	C16—C17—C18—C19	−1.4 (5)
N1—C7—C10—C11	4.1 (6)	C17—C18—C19—O4	0.6 (6)
C8—C7—C10—C11	−171.9 (4)	C16—O4—C19—C18	0.5 (5)

Symmetry codes: (i) −*x*+1, −*y*, −*z*+1; (ii) −*x*+2, −*y*+1, −*z*+1; (iii) −*x*+1, *y*+1/2, −*z*+1/2; (iv) −*x*+2, *y*+1/2, −*z*+1/2; (v) *x*, *y*−1, *z*; (vi) −*x*+1, *y*−1/2, −*z*+1/2.

Hydrogen-bond geometry (Å, º)

D—H···*A*	*D*—H	H···*A*	*D*···*A*	*D*—H···*A*
N1—H1···O2	0.91 (1)	1.72 (3)	2.538 (4)	148 (4)
N2—H2*A*···O3^{vi}	0.91 (1)	2.20 (2)	3.079 (4)	162 (5)

Symmetry code: (vi) −*x*+1, *y*−1/2, −*z*+1/2.